

Improving conditioning of polynomial pole placement problems with application to low-order controller design for a flexible beam

Didier Henrion, Christophe Prieur, Sami Tliba

Abstract—A simple frequency scaling can significantly improve numerical conditioning of the Diophantine equation arising in polynomial pole placement. An application to low-order controller design for active damping of a highly flexible Bernoulli-Euler beam is described.

I. INTRODUCTION

Probably for historical reasons, control engineers generally favor state-space representations to polynomial (transfer function) representations when solving analysis or synthesis problems with the help of computer-aided control system design (CACSD) numerical tools. As pointed out in the recent survey [12], there is a strong bias toward state-space methods. Indeed, it is generally believed that polynomials are always highly sensitive to numerical round-off errors, and therefore cannot be used as reliable modeling objects. As an illustrative example, consider the `numdemo` tutorial and the “Numerical do’s and don’ts” section of the manual of the Control System Toolbox for Matlab [16], where it is recommended to

- stick with the state-space form for all computations;
- use the state-space form for model interconnections;
- compute with the state-space form and avoid combining transfer functions.

Most of the studies in numerical analysis in control focus on state-space methods and real- or complex-valued matrices. Pre-conditioning and balancing techniques such as the LINPACK/LAPACK algorithm implemented in function `ssbal` of the Control System Toolbox have been developed for matrices, but not for polynomials. In general, polynomials are considered as “perfidious” objects which must be avoided as much as possible [29].

We think that it is not justified to favor state-space techniques over polynomial techniques only based on the above observations. State-space problems can be ill-conditioned too, rendering the use of balancing and pre-conditioning techniques necessary. In our opinion there is no solid

theoretical argument to justify why polynomials should be systematically avoided when solving control problems. Moreover, polynomials and polynomial matrices arise naturally when modeling linear systems, and they are generally favored by students because of their clear physical interpretation. Whole branches of control theory dedicated to the polynomial approach [14], [5] and the behavioral approach [21] make extensive use of polynomials and polynomial matrices as modeling objects.

There is undoubtedly a lack of studies on numerical properties of polynomials, which is probably the reason why control engineers generally rely on state-space methods. Preliminary studies on balancing techniques for polynomials were carried out in [27]. Polynomial pseudo-spectra are reliable graphical tools that can be used to study sensitivity of polynomial roots to coefficient perturbations [28], [25]. Pseudo-spectra were used in [30] to study conditioning of polynomials in different bases. Balancing techniques for polynomial representations of linear systems were recently studied in [23]. Note also that some numerically stable linear algebra routines have been designed to solve control problems involving polynomials [8], [22].

In this paper our objective is to study numerical conditioning problems faced when solving pole placement problems by output feedback in the polynomial setting [14]. Most of the studies we are aware of focus on pole placement by state feedback in the state-space setting [19]. In [17], the authors conclude that state-space pole placement is in general ill-conditioned when placing more than 10 poles. They also propose to relax locations of the poles to improve conditioning.

Our study is carried out on the numerical model of a highly flexible Bernoulli-Euler beam equipped with a piezoelectric actuator and a piezoelectric sensor, the kind of systems for which numerical troubles are the most likely to occur. There exists a large literature studying flexible structures in interaction with smart materials. See e.g. [2], [3] for the modeling problem, see e.g. [6] for the control problem and e.g. [7] for the experimental aspects. In this paper we use a model of a smart beam to illustrate our numerical approach. Our method improves the conditioning and allows us to compute a pole placement controller for the flexible structure under consideration.

In Section II, after a brief description of the plant setup, the system model is derived from partial differential equations. In Section III, we study the influence of frequency domain scaling on the conditioning of the linear

D. Henrion is with LAAS-CNRS, 7 Avenue du Colonel Roche, 31077 Toulouse, France. He is also with the Institute of Information Theory and Automation, Academy of Sciences of the Czech Republic, Pod vodárenskou věží 4, 18208 Prague, Czech Republic and with the Faculty of Electrical Engineering, Czech Technical University in Prague, Technická 2, 16627 Prague, Czech Republic. E-mail: henrion@laas.fr

C. Prieur is with SATIE-CNRS, ENS Cachan, 61 Avenue du Président Wilson, 94235 Cachan, France. He is also with LAAS-CNRS, 7 Avenue du Colonel Roche, 31077 Toulouse, France. E-mail: christophe.prieur@satie.ens-cachan.fr

S. Tliba is with SATIE-CNRS, ENS Cachan, 61 Avenue du Président Wilson, 94235 Cachan, France. E-mail: sami.tliba@satie.ens-cachan.fr

system of equations arising when solving the polynomial pole placement Diophantine equation on the beam model. Finally, in Section IV we report our numerical experiments when designing a low-order active damping controller for the beam.

II. MODELING OF THE BERNOULLI-EULER BEAM

Before writing down the model under consideration in this paper, let us motivate our study by describing the experimental setup which is available to check our results.

A. Experimental Setup

In this section we describe the experimental setup with a smart flexible structure.

We consider a flexible cantilever beam, that is clamped at one end and free at the other as shown in Figure 1. Two piezoelectric patches are bonded on this beam. They are placed symmetrically at the root of the beam. One of them is used as sensor and the other is used as actuator.

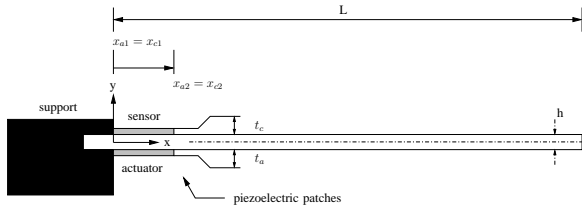


Fig. 1. Flexible cantilever beam

The equipped structure is linked to an experimental device described in Figure 2, allowing a controller implementation on a DSP board.

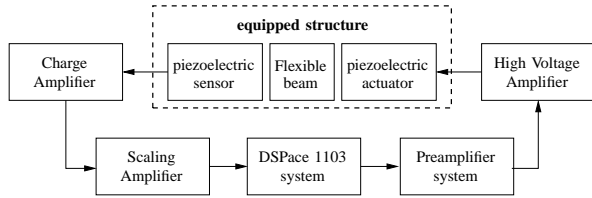


Fig. 2. Experimental setup

At time $t \leq 0$, the beam is submitted to a given strain, the free end is at a distance $w(x = L, t = 0)$ from the equilibrium position as shown in Figure 3. This corresponds to the experiment side of the control problem under study in this paper with the initial conditions defined by (6) : *the controlled beam drop test*.

Let us now give the mathematical model under consideration in this paper to study this control problem.

B. Mathematical model of the beam

We consider a Bernoulli-Euler beam free at one end and clamped at the opposite end. A piezoelectric actuator is attached to the beam. Let us consider the following model

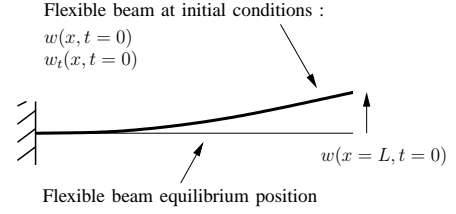


Fig. 3. Flexible beam control problem

written in terms of a partial differential equation [6], [18], [4]:

$$\begin{aligned} w_{tt}(x, t) + \frac{YJ}{\rho A_b} w_{xxxx}(x, t) &= \frac{1}{\rho A_b} m_{xx}(x, t) \\ w(0, t) &= 0, \quad w_x(0, t) = 0 \\ w_{xx}(L, t) &= 0, \quad w_{xxx}(L, t) = 0 \end{aligned} \quad (1)$$

for all (x, t) in $[0, L] \times [0, T]$, where

- $x \in [0, L]$ denotes the spatial coordinate of the beam of length L ,
- $t \in [0, T]$ is the time coordinate,
- $x = 0$ is the clamped boundary of the beam,
- $x = L$ is the free boundary of the beam,
- $w(x, t)$ is the beam transverse deflection at point x and at time t ,
- ρ is the (uniform) density of the beam,
- A_b is the cross-sectional area,
- Y is Young's modulus of elasticity,
- J is the moment of inertia of the beam,
- m is the moment acting on the beam due to the piezoelectric actuator.

The viscous behavior is not considered in (1). It is introduced later in the solution according to the *Basile assumption* (see eg [4]).

The initial conditions are

$$w(x, 0) = w^0, \quad w_t(x, 0) = w^1. \quad (2)$$

The piezoelectric actuator develops a bending moment on the beam due to the applied voltage. This moment is only located under the actuator. It is expressed by

$$m(x, t) = K_a V_a(t) (H(x - x_{a1}) - H(x - x_{a2}))$$

where K_a is a constant based on the properties of the beam and the piezoceramic patches, $V_a(t)$ is the voltage applied to the piezoelectric actuator and $H(x)$ is Heaviside's mapping, i.e. vanishing for all $x < 0$, and equal to 1 for all $x \geq 0$. Here x_{a1} and x_{a2} denote the location of the piezoelectric actuator patch's ends along the x -axis, see [6], [15] for details.

The bending of the beam is measured with a piezoelectric sensor whose voltage is related to the deflection as follows:

$$V_c(t) = K_c \left(\frac{\partial w}{\partial x}(x_{c2}, t) - \frac{\partial w}{\partial x}(x_{c1}, t) \right)$$

where V_c denotes the voltage of the piezoelectric sensor, K_c is a constant based on the properties of the beam. Here

x_{c1} and x_{c2} denote the location of the piezoelectric sensor patch's ends along the x -axis.

The $L^2(0, \pi)$ -normalized modes of partial differential equation (1) are given by

$$\psi_i(x) = \gamma_i (\cos(\alpha_i x) - \cosh(\alpha_i x) + \mu_i (\sinh(\alpha_i x) - \sin(\alpha_i x))) \quad (3)$$

where α_i is the i -th positive root of the equation $1 + \cos(\alpha_i \pi) \cosh(\alpha_i \pi) = 0$, $\mu_i = (\cos(\alpha_i \pi) + \cosh(\alpha_i \pi)) / (\sin(\alpha_i \pi) + \sinh(\alpha_i \pi))$ and $\gamma_i = 1/\sqrt{\pi}$, see e.g. [15], [1] for a proof.

Consider the left-hand side of the first equation in (1), multiply it by ψ_i for a positive integer i and compute the integral over $[0, L]$. We get

$$\begin{aligned} & \int_0^L \frac{1}{\rho A_b} \frac{\partial^2 m}{\partial x^2} \psi_i(x) dx \\ &= \int_0^L \frac{K_a}{\rho A_b} V_a(t) \frac{\partial^2}{\partial x^2} (H(x - x_{a1}) - H(x - x_{a2})) \psi_i(x) dx \\ &= \frac{K_a}{\rho A_b} V_a(t) (\psi_i'(x_{a2}) - \psi_i'(x_{a1})). \end{aligned} \quad (4)$$

Let us consider the N first modal functions and the projection of equation (1) on these spanned space. We now assume that each modal function is equally damped. Defining input $u(t) = V_a(t)$, output $y(t) = V_c(t)$, after application of the Laplace transform we obtain the following SISO finite-dimensional model

$$y(s) = C(s^2 I + sD + E)^{-1} B u(s).$$

The $N \times N$ second-degree denominator polynomial matrix has coefficients

$$D = 2 \operatorname{diag} \zeta_i \omega_i, \quad E = \operatorname{diag} \omega_i^2.$$

where $\zeta_i = 10^{-3}$ are damping factors, $\omega_i = (\alpha_i^2 Y J) / (\rho A_b)$ are modal pulsations, and input and output matrix entries are given by $B_i = K_a / (\rho A_b) (\psi_i'(x_{a1}) - \psi_i'(x_{a2}))$ and $C_i = K_c (\psi_i'(x_{c2}) - \psi_i'(x_{c1}))$ for $i = 1, \dots, N$, see equation (4).

The piezoelectric patches are piezoceramic PZT (see [20, PIC 151]). The experimental beam is in aluminium. The corresponding values of the physical features used both for experimental and numerical purposes are:

- beam density $\rho = 2970 \text{ kg.m}^{-3}$,
- beam thickness $h = 1.58 \cdot 10^{-3} \text{ m}$, beam width $l = 1 \cdot 10^{-2} \text{ m}$, beam length $L = 30 \cdot 10^{-2} \text{ m}$,
- piezoelectric thicknesses $t_a = 4 \cdot 10^{-4} \text{ m}$, $t_c = 4 \cdot 10^{-4} \text{ m}$ for the actuator and the sensor respectively,
- constants of charge $d_{31} = -2.1 \cdot 10^{-10} \text{ V.m}^{-1}$, constant of voltage of the piezoelectric sensor $e_{c31} = -12.358 \text{ V.N}^{-1} \cdot \text{m}^{-1}$, dielectric constant of the piezoelectric sensor $\epsilon_{33}^e = 8.0258 \cdot 10^{-9} \text{ F.m}^{-1}$,
- beam Young's modulus $Y = 7.8 \cdot 10^{10} \text{ Nm}^{-2}$, piezoelectric Young's modulus $Y_a = 8.5 \cdot 10^{10} \text{ Nm}^{-2}$,
- location of the piezoelectric actuator and sensor patches' ends along the x -axis $x_{a1} = x_{c1} = 0 \text{ m}$, $x_{a2} = x_{c2} = 2 \cdot 10^{-2} \text{ m}$.

TABLE I
GAINS, DAMPING COEFFICIENTS AND PULSATIONS FOR DIFFERENT NUMBERS OF FLEXIBLE MODES.

N	k	ζ_i	ω_i	$\hat{\zeta}_i$	$\hat{\omega}_i$
1	-4.5289	10^{-3}	91.315		
2	$-1.4255 \cdot 10^4$	10^{-3}	91.315		
		10^{-3}	572.26	$7.8417 \cdot 10^{-2}$	135.94
3	$-9.7805 \cdot 10^4$	10^{-3}	91.315		
		10^{-3}	572.26	$8.2068 \cdot 10^{-2}$	119.32
		10^{-3}	1602.4	$8.9090 \cdot 10^{-2}$	805.94
4	$-3.3503 \cdot 10^5$	10^{-3}	91.315		
		10^{-3}	572.26	$8.4270 \cdot 10^{-2}$	113.33
		10^{-3}	1602.4	$8.9011 \cdot 10^{-2}$	733.08
		10^{-3}	3140.0	$9.4001 \cdot 10^{-2}$	2139.5
5	$-7.9288 \cdot 10^5$	10^{-3}	91.315		
		10^{-3}	572.26	$8.5562 \cdot 10^{-2}$	110.41
		10^{-3}	1602.4	$8.9346 \cdot 10^{-2}$	704.07
		10^{-3}	3140.0	$9.3145 \cdot 10^{-2}$	2009.0
		10^{-3}	5190.6	$9.6026 \cdot 10^{-2}$	4046.8

Moreover, we have $A_b = hl$, $J = (lh^3)/12$, $K_a = \beta x_{a1}(x_{a1} + 1)/(2(1 + 2\beta x_{a1}(3 + 6x_{a1} + 4x_{a1}^2))) \times d_{a31}lh^2Y/t_a$ where $\beta = Y_a/Y$, $x_{a1} = t_a/h$. We have also $K_c = t_c e_{c31}(h/2 + t_c/2)/(\epsilon_{33}^e(x_{c2} - x_{c1}))$, see [15] or [6] for an alternative formula.

Therefore, the open-loop model of the plant in a transfer function setting is given by

$$\begin{aligned} P(s) &= C(s^2 I + Ds + E)^{-1} B \\ &= k \frac{\prod_{i=2}^N (s^2 + 2\hat{\zeta}_i \hat{\omega}_i + \hat{\omega}_i^2)}{\prod_{i=1}^N (s^2 + 2\zeta_i \omega_i s + \omega_i^2)} \\ &= \frac{b(s)}{a(s)} \end{aligned} \quad (5)$$

where $a(s)$ and $b(s)$ are polynomials of respective degrees $2(N-1)$ and $2N$. Values of the gains, damping coefficients and pulsations are given in Table I for various values of N , the number of flexible modes. The Bode magnitude plot of plant $P(s)$ for $N = 12$ modes is represented in Figure 4.

III. IMPROVING CONDITIONING OF THE POLE PLACEMENT PROBLEM

We want to design a dynamical output feedback controller placing the closed-loop poles of a linear system at desired locations. Given the open-loop plant (5) of order $n_P = 2N$, and a target characteristic polynomial $c(s)$ of degree $n_P + n_K$, we seek a controller

$$K(s) = \frac{q(s)}{p(s)}$$

of order n_K satisfying the polynomial Diophantine equation

$$a(s)p(s) + b(s)q(s) = c(s).$$

If $n_K = n_P - 1$ and $a(s)$ and $b(s)$ are coprime polynomials, a controller satisfying the above equation always exists for any right hand-side $c(s)$ [14]. Finding coefficients of

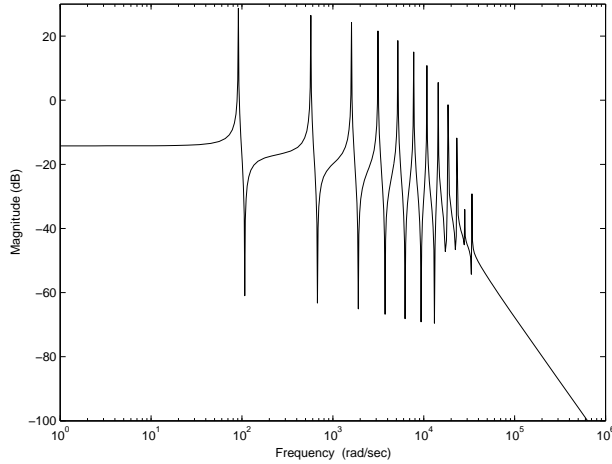


Fig. 4. Bode magnitude plot of the open-loop beam model with $N = 12$ flexible modes.

polynomials $p(s)$ and $q(s)$ then amounts to solving a linear system of equation (LSE)

$$\underbrace{\begin{bmatrix} a_0 & & b_0 & & & \\ & \ddots & & & & \\ & & \ddots & & & \\ a_{n_P} & & a_0 & b_{n_P} & b_0 & \\ & & \ddots & & & \\ & & & \ddots & & \\ & & & & a_{n_P} & b_{n_P} \end{bmatrix}}_S \begin{bmatrix} p_0 \\ \vdots \\ p_{n_K} \\ q_0 \\ \vdots \\ q_{n_K} \end{bmatrix} = \begin{bmatrix} c_0 \\ \vdots \\ c_{n_P+n_K} \end{bmatrix}$$

where S is a non-singular Sylvester matrix of dimension $2n_P$.

In the above LSE, all polynomials are expressed in the standard power basis

$$[1 \quad s \quad s^2 \quad \dots].$$

Obviously, the conditioning of Sylvester matrix S depends on the choice of this basis. Other bases may prove useful in order to minimize the conditioning of S , and hence to solve our pole placement LSE in a more numerically sound way.

For example, choosing

$$[1 \quad \rho s \quad (\rho s)^2 \quad \dots]$$

as an alternate polynomial basis, where ρ is a frequency scaling parameter, we obtain a different Sylvester matrix $S(\rho)$, with a different conditioning. In Figure 5, we represent the conditioning of matrix $S(\rho)$ as a function of ρ for different values of N , the number of flexible modes in the model. We can see that the conditioning of the Sylvester matrix can be greatly improved with a proper choice of ρ .

For example, with $N = 5$ in model (5), the conditioning of $S(1)$ (no scaling) is as large as $3.6 \cdot 10^{42}$ which means that there is no hope to solve the pole placement LSE accurately.

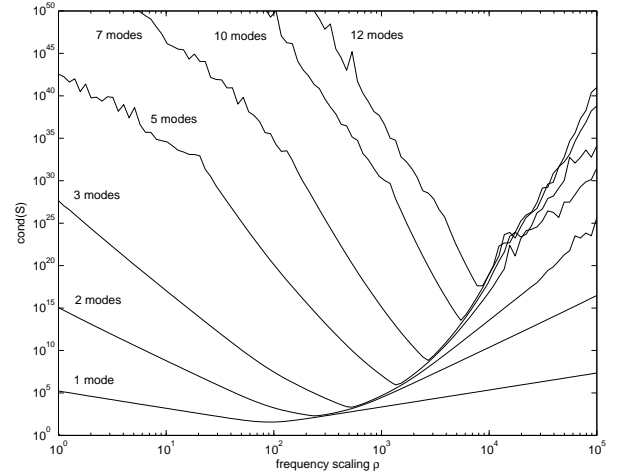


Fig. 5. Conditioning of the Sylvester matrix S as a function of frequency scaling parameter ρ for different numbers of flexible modes.

TABLE II
OPTIMAL FREQUENCY SCALINGS ρ MINIMIZING THE CONDITIONING OF THE SYLVESTER MATRIX $S(\rho)$ FOR N FLEXIBLE MODES.

N	1	2	3	4	5
ρ	91.1	242	509	890	1390
$\log_{10} \text{cond } S(\rho)$	1.6	2.3	3.3	4.6	5.9

However, the conditioning of $S(1390)$ is $8.3 \cdot 10^5$ which is acceptable. In Table II, we report values of ρ minimizing the conditioning of the Sylvester matrices for different values of N . We can notice that there is a relationship between values of ρ and the resonance peaks in Bode diagram (4), see also the pulsations in Table I.

IV. LOW-ORDER CONTROLLER DESIGN BY POLE PLACEMENT

Our closed-loop setup is sketched in Figure 6, where signal X_0 is used to take account of the initial condition. It affects output y through the transfer function

$$\frac{G(s)}{a(s)} = C(s^2 I_N + Ds + E)^{-1}.$$

This initial condition will be used to model a *beam drop test*, i.e. an initial deformation of the beam w^0 , with no initial speed $w^1 = 0$ with the notations of (2).

The closed-loop transfer function from input u to output y is given by

$$T(s) = \frac{b(s)p(s)}{a(s)p(s) + b(s)q(s)}.$$

Specifications of the design problem can be summarized as follows:

- Ensure sufficient damping of the dominating flexible mode(s), by a least a factor ten with respect to the open-loop damping;

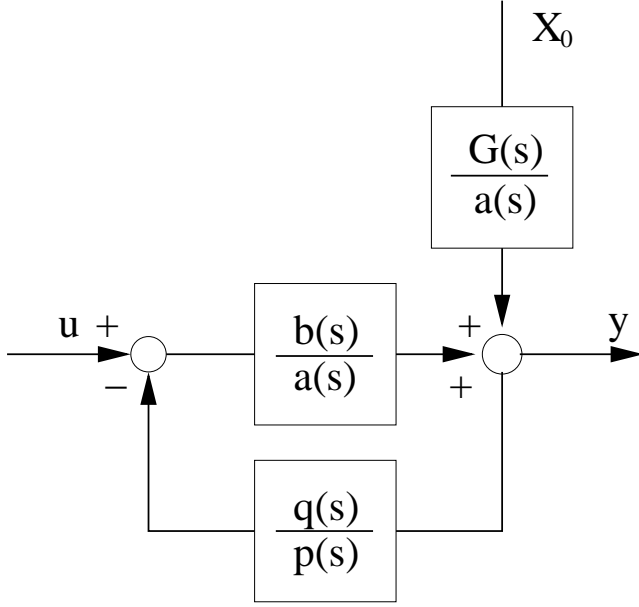


Fig. 6. Closed-loop setup.

- Respect the physical limitations on the input signal, namely $|u(t)| \leq 400$ V.

From Section III, we can design an n_K -th order controller with $n_K = n_P - 1$. However, due to non-singularity of Sylvester matrix S in the pole placement LSE, such a controller is unique for a given target characteristic polynomial. Since we are basically interested in damping the dominating vibrating modes, the controller must preserve the open-loop static gain as much as possible. This implies an additional algebraic constraint $T(0) = P(0)$ which is equivalent to the constraint $q(0) = 0$ on the controller numerator polynomial. To incorporate this additional constraint, we have to increase the order of the controller to $n_K = n_P$.

In other words, the order of the controller is equal to the order of the open-loop plant. Since a low-order controller is generally preferred for physical implementation reasons, we use the following design procedure:

- 1) Choose a low plant order n_P ;
- 2) Design an n_P -th order controller for the n_P -th order plant;
- 3) Analyze the closed-loop performance of the n_P -th order controller;
- 4) If the performance is not satisfactory, increase n_P and go back to step 2.

Starting with $N = 1$ mode for the design plant, the characteristic polynomial to be assigned is as follows:

$$c(s) = (s + \alpha)(s + \beta)(s^2 + 2\zeta\omega s + \omega^2)$$

where α, β are two complex numbers corresponding to the desired controller dynamics, ζ is the desired closed-loop damping coefficient and ω the desired pulsation of the first mode in closed-loop.

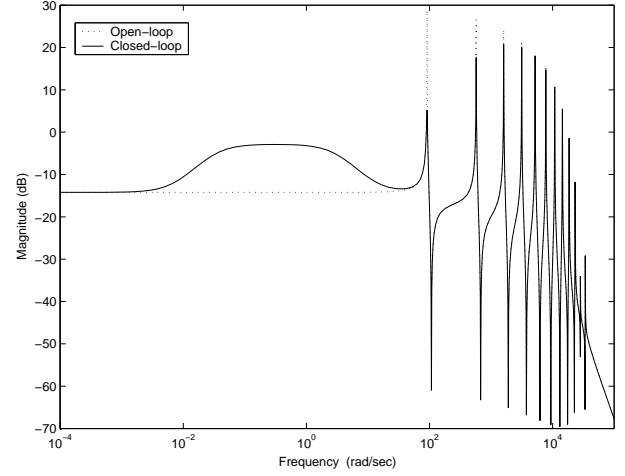


Fig. 7. Compared Bode magnitude plots of the open-loop and closed-loop beam.

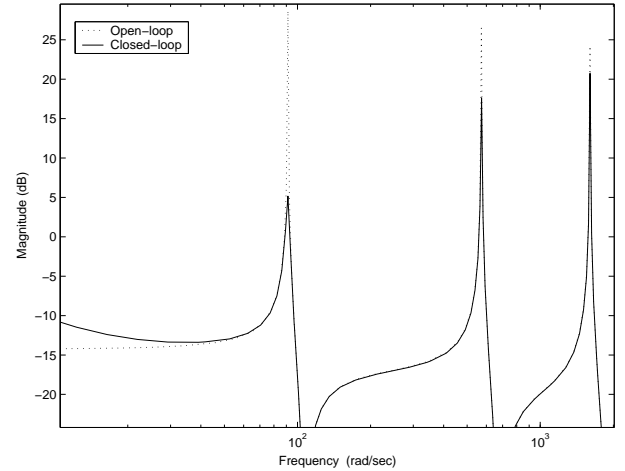


Fig. 8. Compared Bode magnitude plots of the open-loop and closed-loop beam zoomed around the dominant flexible modes.

Following our specifications, we keep $\omega = 91.315$ rad/s as the pulsation of the first mode in open-loop. Our design parameters are then α, β and ζ . Keeping α and β real negative for simplicity, after a series of attempts we used the values $\alpha = -10^{-2}$, $\beta = -10$, $\zeta = 15 \cdot 10^{-3}$ to come up with the following second-order pole placement controller

$$K = \frac{47.075s - 0.055444s^2}{0.10000 + 12.567s + s^2}$$

ensuring damping factors of 15 on the first flexible mode, 2.7 on the second flexible mode, and 1.5 on the third flexible mode. From the magnitude Bode plot of the closed-loop transfer function T shown in Figure 7, we can see the effect of the two parameters α, β , increasing the closed-loop gain

in the low pulsation range. On the zoomed Bode magnitude plot of Figure 8, we can also notice the significant reduction in the resonance peaks of the first, second, and third flexible modes.

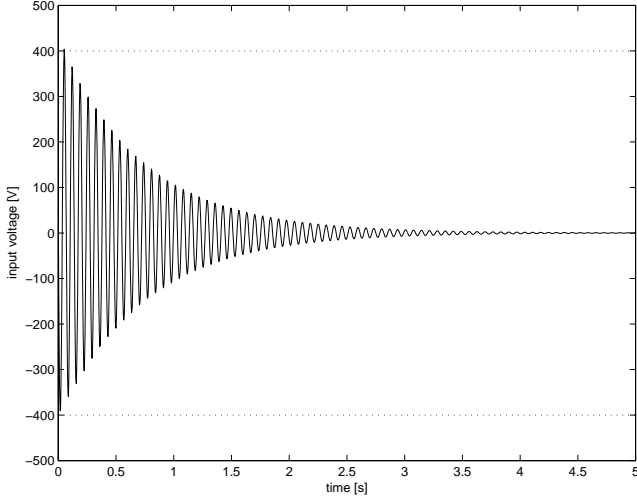


Fig. 9. Time-response of the input voltage.

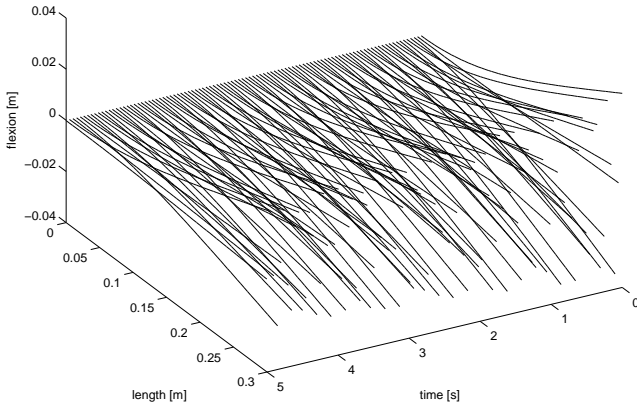


Fig. 10. Profile of the open-loop beam.

Closed-loop simulations were carried out on the setup of Figure 6 with the initial condition $X_0 \in \mathbb{R}^{2N \times 1}$, $X_0 = (10^{-2}, 0, \dots, 0)$. This initial condition correspond to the following initial bending and speed:

$$\begin{aligned} w(x, t = 0) &= 10^{-2} \cdot \psi_1(x), \\ w_t(x, t = 0) &= 0, \end{aligned} \quad (6)$$

where ψ_1 is the first modal function defined by (3). The corresponding deflection is $w(L, t = 0) = 3.5 \cdot 10^{-2}$ m. With this initial condition we simulate an initial deformation of the beam in closed-loop with our pole placement controller, or in open-loop. The beam model used for the simulations has $N = 12$ modes.

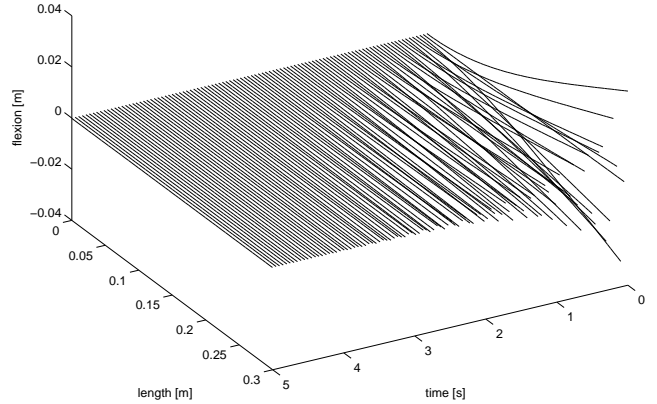


Fig. 11. Profile of the closed-loop beam.

In Figure 9 we can check that the closed-loop input voltage u does not exceed the physical limitation of 400 V.

The profile of the beam, both in open-loop and closed-loop, for 60 time samples in the interval $[0, 5]$ seconds is represented on Figures 10 and 11.

Recall that the above controller was designed based on a plant model with $N = 1$ modes. It turns out that further design experiments on a reference plant with $N = 2, 3 \dots$ modes did not improve significantly the closed-loop performance, while unnecessarily increasing the controller order $n_K = 2N$.

V. CONCLUSION

In the case of polynomial pole placement control for a highly flexible Bernoulli-Euler beam, a physical setup for which CACSD tools are expected to face numerical troubles, it was shown that a simple frequency scaling can significantly improve numerical conditioning.

This study must be considered as a preliminary step towards a more comprehensive synthesis. Our next objective is to design a low-order pole placement controller robust to parametric uncertainty (open-loop damping coefficients and pulsations known within a given range only) and respecting the physical input limitations. Low-order robust polynomial controller design can be carried out with the LMI techniques described in [11]. Even though it was not necessary to resort to Sylvester matrix of large dimensions in the numerical experiments reported in Section IV, it is expected to the pre-conditioning technique exposed in Section III will improve the numerical behaviour of the LMI solver.

Without appropriate scaling or change of basis, it is well-known that linear algebra problems involving polynomials are generally ill-conditioned [29]. This has led researchers to resort systematically to state-space methods, as recalled in [12]. State-space problems can be ill-conditioned too however, and in our opinion there is no solid theoretical background explaining why polynomials should be sys-

tematically avoided when solving control problems. In the control community, there is currently a lack of thorough studies on conditioning properties for polynomials. Alternative polynomial bases (Chebyshev, Bernstein, orthogonal polynomials) can probably help to improve conditioning of the polynomial control problems.

Regarding input limitations, one can either resort to actuator saturation avoidance techniques for which the control law is design explicitly to respect the input constraints [10] and to dynamical input constraints [24], or, alternatively, to robust control techniques where saturations are modeled as additional parametric uncertainties [9].

Finally, we are planning to apply polynomial robust design techniques to MIMO design for active vibration damping of a smart flexible structure using piezoelectric transducers, along the lines described in [26].

ACKNOWLEDGMENTS

We are grateful to Pascal Gahinet for his comments on the balancing algorithm implemented in function `ssbal` of the Control System Toolbox for Matlab, to Andras Varga for his advice on model reduction, and to Adrian Lewis and Michael Overton for discussions on numerical conditioning problems.

REFERENCES

- [1] E. Crépeau, C. Prieur. Control of a clamped-free beam by a piezoelectric actuator. Research report, submitted for publication, 2004.
- [2] P. Destuynder, I. Legrain, L. Castel, N. Richard. Theoretical, numerical and experimental discussion of the use of piezoelectric devices for control-structure interaction. *Eur. J. Mech., A/Solids*, Vol. 11, pp. 97-106, 1992.
- [3] P. Destuynder P. A mathematical analysis of a smart-beam which is equipped with piezoelectric actuators. *Control Cybern.*, Vol. 28, No. 3, pp. 503-530, 1999.
- [4] P. Germain. *Mécanique*. Tome II, Ellipses, Paris, 1996.
- [5] M. J. Grimble, V. Kučera (Eds). *Polynomial methods for control systems design*. Springer Verlag, Berlin, 1996.
- [6] D. Halim, S. O. R. Moheimani. Spatial Resonant Control of Flexible Structures – Applications to a Piezoelectric Laminate Beam. *IEEE Trans. Control Syst. Tech.*, Vol. 9, No. 1, pp. 37–53, 2001.
- [7] D. Halim, S. O. R. Moheimani. Spatial H_2 control of a piezoelectric laminate beam: experimental implementation. *IEEE Trans. Control Syst. Tech.*, Vol. 10, No. 4, pp. 533–546, 2002.
- [8] D. Henrion, M. Šebek. Reliable numerical methods for polynomial matrix triangularization. *IEEE Trans. Autom. Control*, Vol. 44, No. 3, pp. 497–508, 1999.
- [9] D. Henrion, S. Tarbouriech. LMI relaxations for robust stability of linear systems with saturating controls. *Automatica*, Vol. 35, No. 9, pp. 1599–1604, 1999.
- [10] D. Henrion, S. Tarbouriech, V. Kučera. Control of linear systems subject to input constraints: a polynomial approach. *Automatica*, Vol. 37, No. 4, pp. 597-604, 2001.
- [11] D. Henrion, M. Šebek, V. Kučera. Positive polynomials and robust stabilization with fixed-order controllers. *IEEE Trans. Autom. Control*, Vol. 48, No. 7, pp. 1178-1186, 2003.
- [12] N. J. Higham, M. M. Konstantinov, V. Mehrmann, P. H. Petkov. Sensitivity of computational control problems. To appear in the *IEEE Control Systems Magazine*, 2004.
- [13] W. S. Hwang, H. C. Park. Finite element modeling of piezoelectric sensors and actuators. *AIAA Journal*, Vol. 31, No. 5, pp. 930–937, 1993.
- [14] V. Kučera. *Discrete linear control: the polynomial approach*. John Wiley and Sons, Chichester, UK, 1979.
- [15] S. Leleu. Amortissement actif des vibrations d’une structure flexible de type plaque à l’aide de transducteurs piézoélectriques. PhD Thesis, ENS Cachan, France, 2002.
- [16] The MathWorks, Inc. Control System Toolbox for Matlab. Version 5.2.1. Natick, MA, 2002.
- [17] V. Mehrmann, H. Xu. Choosing poles so that the single-input pole placement problem is well-conditioned. *SIAM J. Matrix Anal. Appl.*, Vol. 19, pp. 664–681, 1998.
- [18] L. Meirovitch. *Elements of vibration analysis*. McGraw-Hill, Düsseldorf, 1975.
- [19] P. H. Petkov, N. D. Christov, M. M. Konstantinov. *Computational methods for linear control systems*. Prentice Hall, New York, 1991.
- [20] Physik-Instrumente (PI), *Catalog book*, available at the url <http://www.physikinstrumente.com>, 2004.
- [21] J. W. Polderman, J. C. Willems. *Introduction to mathematical systems theory - A behavioral approach*. Texts in Applied Mathematics, Vol. 26, Springer Verlag, Berlin, 1997.
- [22] PolyX, Ltd. *The Polynomial Toolbox for Matlab. Version 2.5*. Prague, Czech Republic, 2001.
- [23] P. Rapisarda, J. C. Willems. Balanced state representations from higher order differential equations. *Proc. IEEE Conf. on Decision and Control*, Maui, HI, 2003.
- [24] S. Tarbouriech, C. Prieur, J.M. Gomes da Silva Jr, Stability analysis and stabilization of systems presenting nested saturations, Research report, submitted for publication, 2004.
- [25] F. Tisseur, N. J. Higham. Structured pseudospectra for polynomial eigenvalue problems, with applications. *SIAM J. Matrix Anal. Appl.*, Vol. 23, No. 1, pp. 187–208, 2001.
- [26] S. Tliba, H. Abou-Kandil. H_∞ controller design for active vibration damping of a smart flexible structure using piezoelectric transducers. *Proc. IFAC Symp. Robust Control Design*, Milan, Italy, 2003.
- [27] K. C. Toh, L. N. Trefethen. Pseudozeros of polynomials and pseudospectra of companion matrices. *Numerische Mathematik*, Vol. 68, pp. 403–425, 1994.
- [28] L. N. Trefethen. Pseudospectra of linear operators. *SIAM Review*, Vol. 39, pp. 383–406, 1997.
- [29] J.H. Wilkinson. The perfidious polynomial. In: G.H. Golub (Ed.). *Studies in Numerical Analysis, Studies in Mathematics*, Vol. 24, pp. 1–28, Mathematical Association of America, Washington, DC, 1984.
- [30] H. Zhang. Numerical condition of polynomials in different forms. *Elec. Trans. Numer. Anal.* Vol. 12, pp. 66–87, 2001.